

Geophysical Research Letters

RESEARCH LETTER

10.1029/2020GL087649

Key Points:

- Particle-in-cell simulation clearly shows the linear growth and saturation phases of ECH waves
- Simulation demonstrates that heating of cold electrons is negligible and nonresonant
- Simulation suggests that ECH waves saturate by scattering hot electrons into the loss cone

Correspondence to:

X. Tao,
xtao@ustc.edu.cn

Citation:

Wu, Y., Tao, X., Liu, X., Chen, L., Xie, H., Liu, K., & Horne, R. B. (2020). Particle-in-cell simulation of electron cyclotron harmonic waves driven by a loss cone distribution. *Geophysical Research Letters*, 47, e2020GL087649. <https://doi.org/10.1029/2020GL087649>

Received 26 FEB 2020

Accepted 8 APR 2020

Accepted article online 17 APR 2020

Particle-in-Cell Simulation of Electron Cyclotron Harmonic Waves Driven by a Loss Cone Distribution

Yifan Wu^{1,2,3} , **Xin Tao**^{1,2,3} , **Xu Liu**⁴ , **Lunjin Chen**⁴ , **Huasheng Xie**^{5,6} , **Kaijun Liu**⁷ , and **Richard, B. Horne**⁸ 

¹CAS Key Laboratory of Geospace Environment, Department of Geophysics and Planetary Sciences, University of Science and Technology of China, Hefei, China, ²CAS Center for Excellence in Comparative Planetology, Hefei, China,

³Anhui Mengcheng Geophysics National Observation and Research Station, Mengcheng, China, ⁴Department of Physics, University of Texas at Dallas, Dallas, TX, USA, ⁵Hebei Key Laboratory of Compact Fusion, Langfang, China,

⁶ENN Science and Technology Development Co., Ltd., Langfang, China, ⁷Department of Earth and Space Sciences, Southern University of Science and Technology, Shenzhen, China, ⁸British Antarctic Survey, Cambridge, UK

Abstract Electron Cyclotron Harmonic (ECH) waves driven by a loss cone distribution are studied in this work by self-consistent particle-in-cell simulations. These waves have been suggested to play an important role in diffuse auroral precipitation in the outer magnetosphere. However, particle simulation of this instability is difficult because the saturation amplitude of the wave driven by a realistic size loss cone distribution is very small. In this work we use an extraordinarily large number of particles to reduce simulation noise so that the growth and saturation of ECH waves can be investigated. Our simulation results are consistent with linear theory in terms of growth rate, and with observation in terms of wave amplitude. We demonstrate that the heating of cold electrons is negligible and nonresonant, different from previous conclusions, and suggest that the saturation of the wave is caused by the filling of the loss cone of hot electrons.

Plain Language Summary Electron Cyclotron Harmonic (ECH) waves are electrostatic emissions in planetary magnetospheres with typical frequency between harmonics of electron cyclotron frequency. In terrestrial magnetosphere, these waves are believed to cause precipitation of energetic electrons into the atmosphere, forming diffuse aurora in the outer magnetosphere. However, detailed study of the excitation and saturation of the wave is difficult because the wave saturation amplitude driven by a realistic size loss cone distribution is typically below the simulation noise level. Correspondingly, a ring distribution was used in previous numerical studies of the wave. Here we show, by using an extraordinarily large number of simulation particles, the detailed excitation process of ECH waves and the associated electron dynamics. We demonstrate that, different from previous conclusions, the heating of cold electrons is both negligible and nonresonant. We also demonstrate the scattering of hot electrons into the loss cone and suggest that this process leads to the saturation of the wave. This study is useful to the further understanding of the importance of ECH waves in energetic electron dynamics.

1. Introduction

Electron Cyclotron Harmonic (ECH) waves are electrostatic emissions frequently observed in planetary magnetospheres (e.g., Horne et al., 1981; Hospodarsky et al., 2008; Kennel et al., 1970). These emissions typically have frequencies between electron cyclotron frequency harmonics with $\omega \approx (n + 1/2)\Omega_e$, where Ω_e denotes the unsigned electron angular cyclotron frequency and $n \geq 1$ is an integer, representing the harmonic number. Previous studies have suggested that these electrostatic waves can interact strongly with keV electrons and may be responsible for scattering electrons into the atmosphere, resulting in diffuse aurora in the outer magnetosphere (Horne & Thorne, 2000; Ni et al., 2011, 2016; Zhang et al., 2015).

It has long been suggested from linear kinetic theories that the loss cone distribution of electrons could provide the needed region in phase space of positive $\partial f / \partial v_\perp$ to drive ECH waves unstable (Ashour-Abdalla & Kennel, 1978; Fredricks, 1971; Liu et al., 2018; Menietti et al., 2008; Tao et al., 2010; Young et al., 1973; Zhang et al., 2013). Here $f(v_\parallel, v_\perp)$ is the electron phase space density, and v_\parallel and v_\perp are velocity components

parallel and perpendicular to the background magnetic field, respectively. However, particle-in-cell (PIC) simulation of ECH waves driven by a realistic size loss cone distribution is difficult because this instability is very weak (e.g., Umeda et al., 2007). The saturation amplitude of these waves is smaller than the noise level in typical PIC simulations unless an extraordinarily large number of simulation particles are used. To understand the excitation and the related nonlinear processes of ECH waves, previous studies chose to use a ring distribution of hot electrons (Dawson, 1981; Umeda et al., 2007), which makes the instability stronger and therefore easier to simulate. Those studies observed strong resonant heating of cold electrons, which was suggested to be at least partially responsible for the saturation of ECH waves. It is, however, unclear whether the use of a ring distribution changes the physics involved in the generation of ECH waves in realistic magnetospheres.

It is the purpose of this work to investigate the excitation and saturation of ECH waves driven by a loss cone distribution with a realistic loss cone size, together with the associated electron dynamics. The amplitude of ECH waves is a key parameter in quantitatively understanding their roles in electron scattering in the magnetosphere (Horne et al., 1981; Horne & Thorne, 2000; Ni et al., 2011; Zhang et al., 2013); therefore, it is important to understand how these waves saturate. There are several theories about the saturation mechanism of ECH waves. For example, Ashour-Abdalla and Kennel (1978) suggested that ECH waves saturate by a combination of cold electron heating and hot electron precipitation. Using a ring distribution for hot electrons, Dawson (1981) showed that ECH waves saturate by the heating of cold electrons through a type of nonlinear cyclotron resonance and the power provided by hot electrons to waves is essentially balanced by the rate of heating of cold electrons at saturation. Umeda et al. (2007) proposed that both the heating of cold electrons and modification of the hot electron distribution contribute to ECH saturation. Zhang et al. (2013) estimated the saturation amplitude of ECH waves in the framework of quasilinear theory. The exact dynamics of electrons and the saturation mechanism obviously remains to be determined, especially for ECH waves driven by a loss cone distribution.

2. Simulation Results

2.1. Simulation Method and Parameter Setting

In this study, we use a 1-D spatial (x) and 3-D velocity electrostatic PIC code to simulate ECH waves, with x parallel to the direction of wave vector k . From observation, ECH waves propagate almost perpendicular to the background magnetic field. Correspondingly, we choose the wave normal angle $\theta \equiv \langle k, B \rangle = 88.5^\circ$, a typical angle of ECH waves. Two components of electrons are used: a cold component and a hot component. The number density of both components is $n = 1 \text{ cm}^{-3}$. The cold electrons are modeled using a Maxwellian distribution with temperature $T_c = 1 \text{ eV}$. For the hot component, we follow previous studies (e.g., Ashour-Abdalla & Kennel, 1978) to use subtracted Maxwellians to model the loss cone distribution

$$f_h = \frac{1}{(2\pi)^{3/2}v_t^3} \exp\left(-\frac{v_{\parallel}^2}{2v_t^2}\right) \left\{ \Delta \exp\left(-\frac{v_{\perp}^2}{2v_t^2}\right) + \frac{1-\Delta}{1-\beta} \left[\exp\left(-\frac{v_{\perp}^2}{2v_t^2}\right) - \exp\left(-\frac{v_{\perp}^2}{2\beta v_t^2}\right) \right] \right\}, \quad (1)$$

where $v_t = \sqrt{T_h/m}$ is the thermal velocity with $T_h = 500 \text{ eV}$ and Δ and β are the loss cone parameters. Parameter Δ determines the depth of the loss cone, and the distribution reduces to a Maxwellian distribution if $\Delta = 1$. Parameter β largely determines the width of the loss cone. We choose $\Delta = 0$ and $\beta = 0.005$, following previous observational studies (e.g., Horne et al., 2003; Tao et al., 2010), to represent a realistic loss cone distribution of hot electrons in the magnetosphere. These parameters are chosen to roughly represent the plasma conditions in Earth's magnetosphere at $L = 6$, with $B_0 \approx 143.5 \text{ nT}$, and the loss cone angle is about 3° . Note that, different from typical simulation work, we list these parameters in physical units and they are properly normalized before being used in simulation. The distribution of hot electrons can be found in Figure 3a. The ions are fixed, because the frequency of ECH waves is $\sim (n + 1/2)\Omega_e$ with $n \geq 1$, which is much larger than the ion cyclotron frequency.

Figure 1 shows the calculated linear dispersion relation and growth rate using HOTRAY code (Horne, 1989) with these parameters. The linear growth rate suggests that ECH waves with harmonics $n = 1, 2, 3$ are unstable with peak frequencies at $\omega/\Omega_e = 1.56, 2.52$, and 3.28 , respectively, and waves in Band 2 have the largest linear growth rate. The peak growth rates (ω_i/Ω_e) of all three unstable bands are on the order

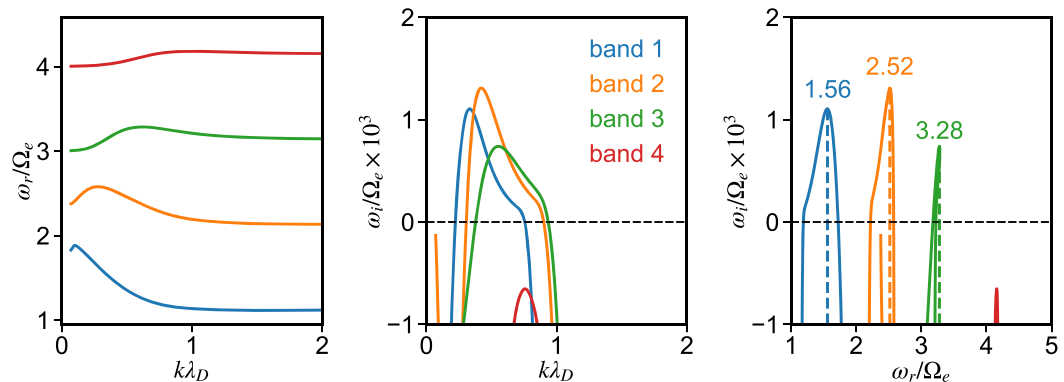


Figure 1. (Left) The linear dispersion relation of ECH waves for parameters in this study. (Middle) The linear growth rate as a function of k . (Right) The linear growth rate as a function of wave frequency ω_r . Vertical dashed lines mark the locations of maximum linear growth rate of the corresponding band.

of $\mathcal{O}(10^{-3})$ with $k\lambda_D \sim 0.5$ and λ_D the Debye length of cold electrons. The corresponding frequency of maximum ω_i is near $(n + 1/2)\Omega_e$ with $n = 1, 2, 3$ consistent with observations.

From the linear growth rate calculation that $k\lambda_D(\omega_{i,\max}) \approx 0.5$ for all three bands, we choose the simulation cell size to be $\Delta x = 0.76\lambda_D$ and use in total 128 cells. Therefore, the length of the simulation domain L is roughly eight times the wave length of the most unstable modes in all three bands. The cell size is smaller than λ_D to avoid unphysical heating. The simulation time step is $t\Omega_e = 0.02$ to properly resolve the gyromotion of electrons. ECH wave instability driven by a loss cone distribution is very weak in the sense that their saturation amplitude is smaller than the noise level in typical PIC simulations. To accurately model the saturation of wave field, one needs to use a large number of simulation particles to bring down the noise. To find the appropriate number of particles, we tried several runs of simulation, and each time, we double the number of simulation particles until the saturation amplitude essentially does not change. This indicates that the saturation amplitude in simulation is physical and higher than the noise level because statistical noise decreases with increasing number of particles. We end up using 1,600,000 particles per cell.

2.2. Energy Evolution and Wave Properties

Figure 2 shows the evolution of field and particle energy density, and the wave power spectral density. The electric field energy density (Figure 2a) increases from about 10^{-10} at $t\Omega_e = 0$ to about 10^{-9} at $t\Omega_e = 1,600$; therefore, the average growth rate is $\bar{\gamma}/\Omega_e \approx 7.2 \times 10^{-4}$, consistent with linear theory calculation. A more detailed analysis of wave growth rate will be given in section 2.4. At $t\Omega_e \sim 2,000$, the average wave intensity $\langle \delta E^2 \rangle$, normalized by B_0^2 because of the use of Gaussian units in simulation, saturates near 1.5×10^{-9} (or $\langle \delta E^2 \rangle/n_h T_{h0} = 4 \times 10^{-6}$ with $T_{h0} = 500$ eV). Correspondingly, the average wave saturation amplitude is about $4 \times 10^{-5} B_0$, or 1.7 mV/m with $B_0 = 143.5$ nT. This value is consistent with typical amplitude of ECH waves from satellite observation, which is on the order of 1 mV/m during active times (e.g., Meredith et al., 2009; Ni et al., 2011). The evolution of cold electrons, hot electrons, and the total particle energy density is plotted together with the wave energy density in Figure 2b. The energy density of cold (hot) electrons increases (decreases) until about $t\Omega_e \sim 3,000$ and stays at a roughly constant level thereafter. The difference in the saturation time of the average wave intensity $\langle \delta E^2 \rangle$ and the electron energy density is due to the fact that $\langle \delta E^2 \rangle$ represents the summation of intensity of all excited modes. Each individual wave mode, however, may saturate at different times and continuously exchange energy with electrons after saturation, as can be seen in Figure 4. The total particle energy density is always balanced by the wave energy density, showing good energy conservation of the simulation code. The parallel and perpendicular temperature evolution of cold and hot electrons is presented in Figure 2c. Here the direction is defined with respect to the background magnetic field. The most significant change of temperature occurs in the perpendicular direction for both cold and hot electrons, which is related to the nearly perpendicular propagation direction of ECH waves. Similar to the energy evolution profile, perpendicular temperature of hot (cold) electrons decreases (increases) until $t\Omega_e \sim 3,000$, but only by about $10^{-6} T_{h0}$ ($10^{-3} T_{c0}$). The amount of heating of cold and hot electrons here is completely different from previous simulation results using a ring distribution. For example, in the study of Umeda et al. (2007), $\Delta T_h/T_{h0} \sim \mathcal{O}(10^{-1})$, and $\Delta T_c/T_{c0} \sim \mathcal{O}(10)$. More detailed discussion

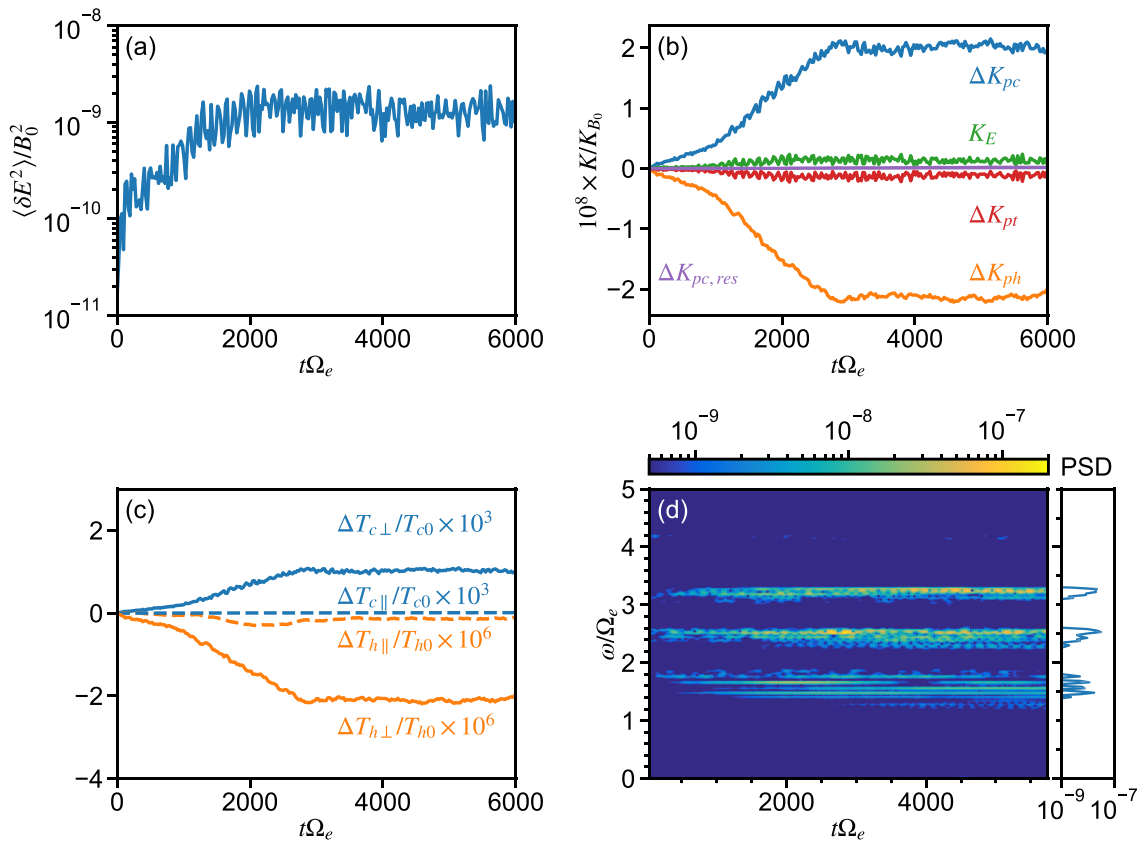


Figure 2. (a) The evolution of averaged wave intensity. (b) The change of energy densities of wave electric field ($K_E \equiv \langle \delta E^2 \rangle / 8\pi$), cold electrons (ΔK_{pc}), hot electrons (ΔK_{ph}), all electrons ($\Delta K_{pt} = \Delta K_{pc} + \Delta K_{ph}$), and all potentially resonant cold electrons ($\Delta K_{pc,res}$). These values are normalized by the energy density of background magnetic field, $K_{B_0} \equiv B_0^2 / 8\pi$. (c) The change of cold and hot electron temperature in perpendicular and parallel directions. (d) The frequency-time spectrogram showing three bands of ECH waves. The time-averaged wave power spectral intensity (PSD) as a function of frequency is shown as the side panel.

is given in the next section. The spectrogram of the wave field is presented in panel (d), which clearly shows three bands of ECH waves. The peak frequencies of the time-averaged PSD are at $1.48\Omega_e$, $2.53\Omega_e$, and $3.27\Omega_e$, consistent with linear theory prediction. The root mean squared wave amplitude, obtained by integrating wave power spectral density over frequency, is about $1.75 \times 10^{-5}B_0$, $2.04 \times 10^{-5}B_0$, and $1.82 \times 10^{-5}B_0$ for Bands 1, 2, and 3, respectively. The comparable wave amplitude suggests that all three bands of ECH waves are equally important in the wave-particle interactions and scattering hot electrons into the loss cone.

2.3. The Nonresonant Heating of Cold Electrons

One of the main conclusions reached by previous PIC simulations of ECH waves with a ring distribution is that cold electrons could be resonantly heated, and this process plays an important role in the saturation of ECH waves (Dawson, 1981; Umeda et al., 2007). The energy and temperature evolution of cold electrons, presented in Figure 2, suggests that this might not be the case when a loss cone distribution is used. In this section, we isolate cold electrons that can resonantly interact with ECH waves in simulation and quantitatively calculate their energy density. If the energy density change of this portion of electrons dominates the cold electron energy density change, then the heating of cold electrons is a resonant process; otherwise, it is nonresonant.

We identify resonant electrons in two steps. First, we calculate resonant velocities as $v_r = (\omega - n\Omega_e)/k_{\parallel}$, where $k_{\parallel} = k \cos \theta$ and n is the order of cyclotron resonance. Using k_{\parallel} obtained from linear dispersion relation, and $1.19 \leq \omega/\Omega_e \leq 1.72$, $2.22 \leq \omega/\Omega_e \leq 2.58$, and $3.18 \leq \omega/\Omega_e \leq 3.28$ for three bands, we find that the minimum resonant velocity is $v_r/c \approx 0.0058$, which is resonant velocity of the third band with $n = 3$. Then, we estimate a trapping width Δv_{\parallel} using the wave amplitude in simulation, since all electrons within $v_r \pm \Delta v_{\parallel}$ can approximately resonate with the wave. From Lichtenberg and Lieberman (1983, pp. 122–123),

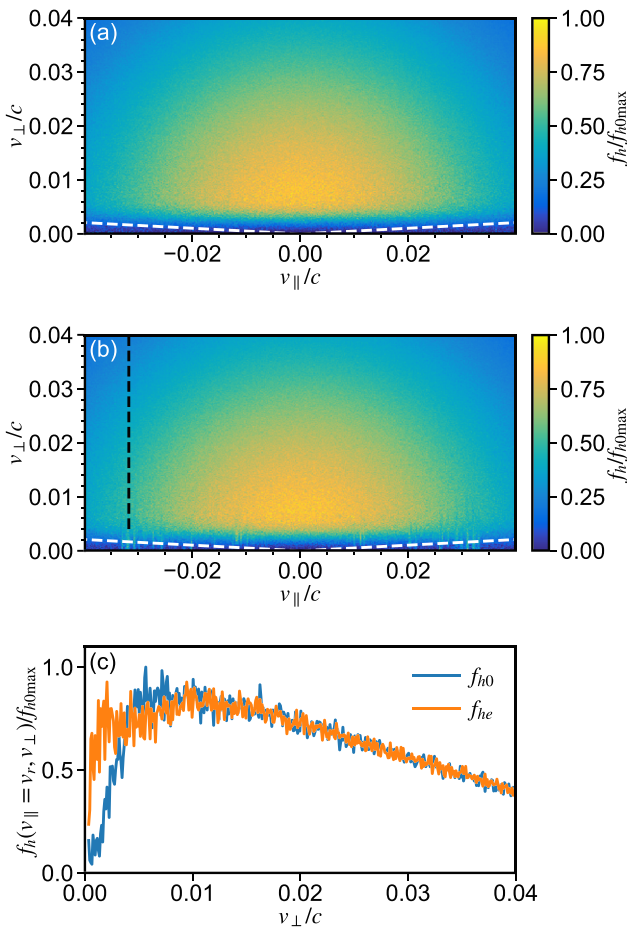


Figure 3. (a) Initial phase space density of hot electrons, and the white dashed lines mark a loss cone of 3° angle to help visualization. (b) Phase space density of hot electrons at saturation stage, while the black dashed line denotes the velocity satisfying $n = 2$ cyclotron resonance with the wave mode of maximum linear growth rate in the 1_{st} band. (c) Initial and final phase space densities as a function of v_{\perp} at the resonant velocity marked in (b).

the trapping frequency of particles resonantly interacting with an obliquely propagating electrostatic wave near the n_{th} order resonance is

$$\omega_{tr} = \sqrt{\frac{e\Phi_0 J_n k^2}{m}}. \quad (2)$$

Here Φ_0 is amplitude of the electrostatic potential of the perturbation, and J_n is the n th-order Bessel function of the first kind with argument $k_{\perp}\rho$, where ρ is the electron cyclotron radius and $k_{\perp} = k \sin \theta$. Since the amplitude of the electric field parallel to B is $\delta E_{\parallel} = \Phi_0 k_{\parallel}$, the trapping frequency can be rewritten using δE_{\parallel} as

$$\omega_{tr} = \sqrt{\frac{e\delta E_{\parallel} J_n k_{\parallel}}{m}}. \quad (3)$$

We then may roughly estimate the half width of resonant v_{\parallel} as

$$\Delta v_{\parallel} = \frac{2\omega_{tr}}{k_{\parallel}} \leq 2\sqrt{\frac{e\delta E_{\parallel}}{k_{\parallel} m}} = 2\sqrt{\frac{e\delta E_0}{km}}, \quad (4)$$

where δE_0 is the amplitude of the ECH wave, and we used the fact that $|J_n| \leq 1$. To obtain the amplitude of each band in simulation, we integrate the wave PSD in $1 \leq \omega/\Omega_e \leq 2$, $2 \leq \omega/\Omega_e \leq 3$, and $3 \leq \omega/\Omega_e \leq 4$ to roughly estimate δE_0^2 for each band, and the result is $\delta E_0/B \simeq 2.1 \times 10^{-5}$, 2.5×10^{-5} , and 1.8×10^{-5} , respectively. The linear dispersion relation gives k for each band: $k\lambda_D \simeq 0.39$, 0.40 , and 0.56 . Therefore, we get $\Delta v_{\parallel}/c \sim 3.7 \times 10^{-4}$, 3.9×10^{-4} , and 2.8×10^{-4} . In simulation, we calculate the energy change of all cold electrons with $v_{\parallel}/c \geq 0.005$, which includes all possibly resonant cold electrons (about 0.02% of all cold electrons). As demonstrated in Figure 2b, the energy change of this portion of cold electrons is less than 1% of that of all cold electrons. Correspondingly, the overall heating of cold electrons is nonresonant, different from the results of Dawson (1981) and Umeda et al. (2007). Most cold electrons merely oscillate nonresonantly in the excited wave field. Thus, the saturation of ECH waves cannot be caused by heating of cold electrons, but more possibly due to exhausting free energy of hot electrons. To investigate the possible saturation mechanism of ECH waves, we study the evolution of hot electron distribution.

2.4. Evolution of the Hot Electron Distribution Function and Wave Dispersion Relation

Figure 3 shows the hot electron distributions at initial and final stages. The initial distribution of hot electrons, presented in Figure 3a, is a loss cone distribution. The size of the loss cone is about 3°, as indicated by the dashed line. The distribution at saturation is similar to the initial distribution, except for the many nearly vertical stripes inside the loss cone. This corresponds to the scattering of hot electrons into the loss cone by the excited ECH waves. These velocities are resonant velocities of generated ECH waves. For example, for the first band of ECH wave, with the frequency of maximum PSD in Figure 2d and the dispersion relation in Figure 1, we obtain $v_r = -0.0318c$. This velocity is marked in Figure 3b as the black vertical dashed line, and it is well consistent with where the loss cone is filled (note the vertical stripes on the plot). In Figure 3c, we show the one-dimensional distribution function at $v_{\parallel} = v_r = -0.0318c$. It is clear that, due to scattering by ECH waves, the loss cone is gradually filled and f_h significantly increases inside the loss cone. Note that the discreteness of v_r of scattered electrons in the loss cone is related to the discreteness of k in our simulation. With a more continuous wave spectrum of ECH waves in observation, we would expect the precipitating electron energy spectrum to be also continuous. We do not show the distribution evolution of cold electrons, because the change of f_c is negligible.

Previous studies using a ring distribution of hot electrons suggested that the significant heating of cold and hot electrons modifies the dispersion relation of ECH waves, which contribute to wave saturation (Umeda

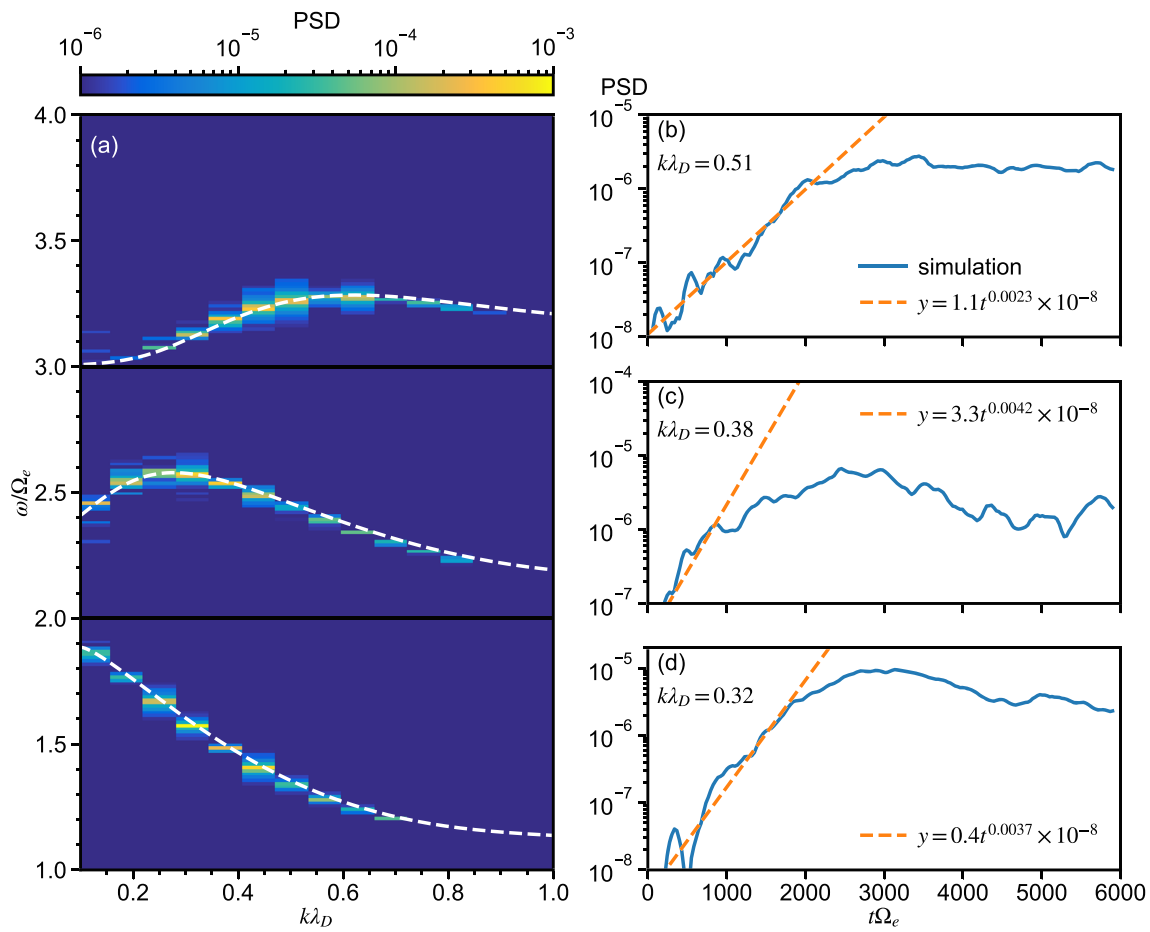


Figure 4. (a) Dispersion relation of ECH waves at the end of simulation obtained using 2-D FFT. The white dashed curves denote the dispersion relation obtained from linear theory with initial plasma parameters. The evolution of wave PSD of the modes with maximum linear growth rate in the third, second, and first bands is shown in panels (b), (c), and (d), respectively. The orange dashed lines are fitting results using the initial values of wave PSD, from which initial growth rates are estimated.

et al., 2007). Here in Figure 4, we investigate the wave dispersion relation at saturation stage and the evolution of wave intensity of modes with maximum linear growth rate in the first three bands. The wave dispersion relation from simulation is obtained from 2-D FFT of wave electric fields near the end of simulation ($5,508 \leq t\Omega_e \leq 6,000$). Its comparison with linear theory calculation using initial parameters proves that the dispersion relation of ECH waves remains essentially unchanged, which is related to the negligible heating of electrons in our case. Using a moving window 2-D FFT, we obtain the evolution of intensity of the modes of maximum linear growth rate in the three bands of waves, shown in Figures 4b–4d. Fitting the wave PSD as a function of time gives an estimate of the initial growth rate, which is 1.85×10^{-3} , 2.1×10^{-3} , and 1.15×10^{-3} for Bands 1, 2, and 3, respectively. These values agree with linear theory predictions (Figure 1b) within about a factor of 2. Figure 4 also shows that as the loss cone is filled by scattered hot electrons, the wave growth rates start to decrease, and different modes reach saturation ($\gamma \sim 0$) at different times. For example, for the mode in Band 2 (Figure 4c), the growth rate γ deviates from the initial value from $t\Omega_e \approx 1,000$ and reaches 0 near $t\Omega_e \approx 2,500$. The other two modes behave similarly, except with different saturation times. The decay of the modes in Bands 1 and 2 (Figures 4c and 4d) represents the change of electron distribution from wave-particle interactions and suggests that some wave energy is transferred back to electrons. From these results, we conclude that ECH waves generated by a loss cone distribution saturate by scattering hot electrons into the loss cone, which reduces $\partial f / \partial v_\perp$. This conclusion is different from the case where a ring distribution is used, as demonstrated by Umeda et al. (2007).

3. Conclusion and Discussion

In this study, we presented 1-D PIC simulations of ECH wave instability driven by a realistic size loss cone distribution. As far as we are aware of, this is the first simulation study about ECH waves driven unstable by a loss cone distribution. We use an extraordinarily large number of particles to bring down the simulation noise, and, therefore, the linear growth phase and wave saturation can be clearly demonstrated. The growth rate from simulation is consistent with linear theory prediction, and the saturation amplitude is also consistent with observation.

We carefully investigated the heating of cold electrons and demonstrated that this process is nonresonant and temperature increase of cold electrons is negligibly small, probably because of the small wave amplitude. This conclusion is significantly different from previous results by Dawson (1981) and Umeda et al. (2007), who studied ECH waves excited by a ring distribution and observed significant resonant heating of cold electrons. We conclude that cold electrons oscillate nonresonantly back and forth in the excited wave field. This kind of particle energy is typically considered as part of the wave energy in plasma wave theory (e.g., Stix, 1992).

We then studied the evolution of hot electron distribution function and wave dispersion relation. We found that excited ECH waves can scatter hot electrons into the loss cone and this scattering occurs at resonant velocities of excited wave modes. The scattered electrons fill up the loss cone and in turn reduce the growth rate of ECH waves. Therefore, we suggest that ECH waves saturate by reducing $\partial f / \partial v_{\perp}$ inside the loss cone and therefore exhausting free energy of hot electrons. On the other hand, the dispersion relation of ECH waves remains almost the same, different from the ring distribution simulation results (Umeda et al., 2007).

Our results about the heating of cold electrons and the saturation process of ECH waves are significantly different from previous studies with a ring distribution of hot electrons (Dawson, 1981; Umeda et al., 2007). We therefore conclude that it is important to use realistic distributions of electrons to study ECH instability to obtain conclusions that are relevant to observations.

Acknowledgments

This work was supported by NSFC grants (41674174, 41631071, 41474142, and 41974168), the Fundamental Research Funds for the Central Universities, the B-type Strategic Priority Program of the Chinese Academy of Sciences (Grant XDB41000000), and UK National Environment Research Council Highlight Topic Grant NE/P10738X/1 (Rad-Sat). Simulation data can be downloaded online (from <http://doi.org/10.5281/zenodo.3679092>).

References

- Ashour-Abdalla, M., & Kennel, C. F. (1978). Nonconvective and convective electron cyclotron harmonic instabilities. *Journal of Geophysical Research*, 83(A4), 1531–1543.
- Dawson, J. M. (1981). Simulation of space plasma phenomena. In S. Akasofu & J. Kan (Eds.), *Physics of auroral arc formation* (Vol. 25, pp. 270–282). Washington DC: American Geophysical Union (AGU). <https://doi.org/10.1029/GM025p0270>
- Fredricks, R. W. (1971). Plasma instability at $(n+1/2)f_c$ and its relationship to some satellite observations. *Journal of Geophysical Research*, 76, 5344–5348. <https://doi.org/10.1029/JA076i022p05344>
- Horne, R. B. (1989). Path-integrated growth of electrostatic waves: The generation of terrestrial myriametric radiation. *Journal of Geophysical Research*, 94(A7), 8895–8909.
- Horne, R. B., Christiansen, P. J., Gough, M. P., Rönnmark, K., Johnson, J. F. E., Sojka, J., & Wrenn, G. L. (1981). Amplitude variations of electron cyclotron harmonic waves. *Nature*, 294, 338–340.
- Horne, R. B., & Thorne, R. M. (2000). Electron pitch angle diffusion by electrostatic electron cyclotron harmonic waves: The origin of pancake distributions. *Journal of Geophysical Research*, 105(A3), 5391–5402.
- Horne, R. B., Thorne, R. M., Meredith, N. P., & Anderson, R. R. (2003). Diffuse auroral electron scattering by electron cyclotron harmonic and whistler mode waves during an isolated substorm. *Journal of Geophysical Research*, 108(A7), 1290. <https://doi.org/10.1029/2002JA009736>
- Hospodarsky, G. B., Averkamp, T. F., Kurth, W. S., Gurnett, D. A., Menietti, J. D., Santolik, O., & Dougherty, M. K. (2008). Observations of chorus at Saturn using the Cassini Radio and Plasma Wave Science instrument. *Journal of Geophysical Research*, 113, A12206. <https://doi.org/10.1029/2008JA013237>
- Kennel, C. F., Scarf, F. L., Fredricks, R. W., McGehee, J. H., & Coroniti, F. V. (1970). VLF electric field observations in the magnetosphere. *Journal of Geophysical Research*, 75(31), 6136–6152. <https://doi.org/10.1029/JA075i031p06136>
- Lichtenberg, A., & Lieberman, M. (1983). *Regular and Chaotic Dynamics* (second). New York: Springer Verlag.
- Liu, X., Chen, L., Gu, W., & Zhang, X. J. (2018). Electron cyclotron harmonic wave instability by loss cone distribution. *Journal of Geophysical Research: Space Physics*, 123, 9035–9044. <https://doi.org/10.1029/2018JA025925>
- Menietti, J. D., Santolik, O., Rymer, A. M., Hospodarsky, G. B., Persoon, A. M., Gurnett, D. A., et al. (2008). Analysis of plasma waves observed within local plasma injections seen in Saturn's magnetosphere. *Journal of Geophysical Research*, 113, A05213. <https://doi.org/10.1029/2007JA012856>
- Meredith, N. P., Horne, R. B., Thorne, R. M., & Anderson, R. R. (2009). Survey of upper band chorus and ECH waves: Implications for the diffuse aurora. *Journal of Geophysical Research*, 114, A07218. <https://doi.org/10.1029/2009JA014230>
- Ni, B., Thorne, R. M., Horne, R. B., Meredith, N. P., Shprits, Y. Y., Chen, L., & Li, W. (2011). Resonant scattering of plasma sheet electrons leading to diffuse auroral precipitation: 1. Evaluation for electrostatic electron cyclotron harmonic waves. *Journal of Geophysical Research*, 116, A04218. <https://doi.org/10.1029/2010JA016232>
- Ni, B., Thorne, R. M., Zhang, X., Bortnik, J., Pu, Z., Xie, L., et al. (2016). Origins of the Earth's diffuse auroral precipitation. *Space Science Reviews*, 200(1-4), 205–259. <https://doi.org/10.1007/s11214-016-0234-7>
- Stix, T. H. (1992). *Waves in Plasmas*. College Park, Maryland: American Institute of Physics.

- Tao, X., Thorne, R., Horne, R. B., Grimald, S., Arridge, C. S., Hospodarsky, G. B., et al. (2010). Excitation of electron cyclotron harmonic waves in the inner Saturn magnetosphere within local plasma injections. *Journal of Geophysical Research*, 115, A12204. <https://doi.org/10.1029/2010JA015598>
- Umeda, T., Ashour-Abdalla, M., Schriver, D., Richard, R. L., & Coroniti, F. V. (2007). Particle-in-cell simulation of Maxwellian ring velocity distribution. *Journal of Geophysical Research*, 112, A04212. <https://doi.org/10.1029/2006JA012124>
- Young, T. S. T., Callen, J. D., & McCune, J. E. (1973). High-frequency electrostatic waves in the magnetosphere. *Journal of Geophysical Research*, 78, 1082–1099. <https://doi.org/10.1029/JA078i007p01082>
- Zhang, X., Angelopoulos, V., Ni, B., & Thorne, R. M. (2015). Predominance of ECH wave contribution to diffuse aurora in Earth's outer magnetosphere. *Journal of Geophysical Research: Space Physics*, 120, 295–309. <https://doi.org/10.1002/2014JA020455>
- Zhang, X., Angelopoulos, V., Ni, B., Thorne, R. M., & Horne, R. B. (2013). Quasi-steady, marginally unstable electron cyclotron harmonic wave amplitudes. *Journal of Geophysical Research: Space Physics*, 118, 3165–3172. <https://doi.org/10.1002/jgra.50319>